17th World Conference on Earthquake Engineering, 17WCEE

Sendai, Japan - September 13th to 18th 2020

IMPACT OF SAMPLING TECHNIQUES ON UNCERTAINTY PROPAGATION WITH NON-LINEAR DYNAMIC ANALYSIS

A. Miano[(1)], H. Ebrahimian[(2)], F. Jalayer[(3)], D. Vamvatsikos[(4)], A. Prota[(5)]

[(1)] *Post-doctoral Scholar, University of Naples Federico II, andrea.miano@unina.it*
[(2)] *Assistant Professor, University of Naples Federico II, ebrahimian.hossein@unina.it*
[(3)] *Associate Professor, University of Naples Federico II, fatemeh.jalayer@unina.it*
[(4)] *Assistant Professor, National Technical University of Athens, divamva@mail.ntua.gr*
[(5)] *Full Professor, University of Naples Federico II, aprota@unina.it*

Abstract

The Method:

Quantifying the impact of modelling uncertainty on the seismic performance assessment is a crucial issue for existing buildings, considering the partial information available related to material properties, construction details and the uncertainty in the capacity models. It has been proved that the effect of structural modelling uncertainties on the seismic performance of existing buildings can be comparable to that of uncertainty in ground motion representation. In this work, the impact of different sampling techniques such as Standard Monte Carlo simulation and Latin Hypercube sampling with Simulated Annealing on the uncertainty propagation with non-linear dynamic analysis has been investigated. Two alternative non-linear dynamic analysis procedures, namely, Incremental Dynamic Analysis and Cloud Analysis are explored. The types of uncertainty encompass record-to-record variability, structural modelling parameters and the fragility model parameters. A one-to-one sampling approach has been adopted in which each of the ground motion records is paired up with a different realization of the structural model.

The Application:

The case-study structure consists of three stories with a semi-embedded story. The structure lies on soil type B (according to national Italian code NTC 2018 site classification). The building is constructed in the 1960s and is designed for gravity loads only. The structure is composed of bi-dimensional parallel frames, without transversal beams. The main central frame in the structure is used herein as structural model. The finite element model of the frame is constructed, using OpenSees, assuming that the non-linear behaviour in the structure is modelled as distributed plasticity. The Beam-with-hinges element from the library of OpenSees is used to model the distributed plasticity. As the uniaxial material from OpenSees library, Pinching4 Material is used. The points on the backbone curve are defined as cracking, yielding, spalling and the ultimate, respectively. These points are obtained based on moment-curvature analysis of beam-column elements subjected to flexure and axial force. The lateral force-deformation response of the element is obtained by considering as a spring the flexural-compression response of the element (section analysis for normal stresses) which is acting in series with a shear spring and a spring representing the fixed-end rotations. The total lateral force deformation response of the element considers the interaction between the shear, bar-slip and the axial-flexural response. A large ground motion set of 160 records from NGA West2 Database, ITACA (Italian Accelerometric Archive), and recent Iranian recordings (International Institute of Earthquake Engineering, IIEES, personal communication) has been employed. Cloud Analysis and IDA have been implemented with the complete set of 160 un-scaled records. Moreover, Cloud Analysis and IDA have been carried out with sub-sets of respectively 50 and 30 ground motion records.

Keywords: Performance-based design; RC buildings; epistemic uncertainties; Latin Hypercube Sampling; Monte Carlo

1. Introduction

Assessment of analytical structural fragility for existing buildings is one of the fundamental steps in the modern performance-based engineering [1]. One main feature distinguishing the assessment of existing buildings from that of the new ones is the amount of uncertainty present in determining the structural modeling parameters. Considering the partial information available related to material properties, construction details and also the uncertainty in the capacity models, the impact of modelling uncertainties on the seismic performance assessment can be critical for existing buildings. Thus, explicit consideration of modelling uncertainty in the assessment of the structural performance for existing buildings can lead to more accurate results.

In order to assess the performance of existing buildings, there are alternative non-linear dynamic analysis procedures available in the literature. In this work, two methodologies, namely Modified Cloud Analysis (MCA) [2] and Incremental Dynamic Analysis (IDA) [3, 4], are employed to characterize the fragility, expressed as the conditional probability of exceeding a prescribed limit state given the seismic intensity. The Cloud Analysis (CA) [5-7] involves the non-linear analysis of the structure subjected to a set of un-scaled ground motion time-histories. CA is based on a few simplifying assumptions (fixed standard error of regression, mean response varying linearly as a function of intensity measure, *IM*, in the logarithmic scale, and structural response given *IM* being modeled as a lognormal distribution), and can be sensitive to the selected suite of records [2, 6]. MCA considers also the global collapse cases (i.e., the numerical non-convergence and/or global dynamic instability in the nonlinear dynamic analysis, see [2]), based on coupling the linear regression in the logarithmic space of structural response versus *IM* for a suite of registered records (i.e., CA) with logistic regression on the collapse and non-collapse part of the Cloud data. IDA involves the prediction of structural demand (often measured in terms of maximum inter-story drift ratio) for a suite of ground motions, scaled successively to higher *IM* levels. MCA and IDA have been largely used in the literature, not only to model the record-to-record (R2R) variability in ground motion, but also to propagate structural modelling uncertainties. These uncertainties can be categorized as uncertainties in component capacities, the uncertainties in mechanical material properties, and construction details [8-14].

Herein, the nonlinear dynamic analysis procedures rely on adopting a critical demand to capacity ratio as the damage measure, which is equal to unity at the onset of limit state [15]. This provides the possibility of identifying the limit state exceedance in the component level and map it to the structural level, and considers the correlation between demand and capacity. Simulation-based methods are arguably the most efficient way for taking into account the epistemic uncertainties (see e.g., [13-14]). For generating different realization of structural model in this study, we employed the standard Monte Carlo Simulation (MCS) and the Latin Hypercube Sampling (LHS) with Simulated Annealing procedure [16]. Each record is applied to a different realization of the structural model (i.e., the one-to-one assignment; see [14, 17]); note that the number of structural analyses is equal to the number of records; which in turn is equal to the number of structural model realizations. To take into account the uncertainty in the fragility model parameters, a Bayesian updating framework, denoted as Robust fragility [2] is adopted, which treats the structural response to the selected records as “data”. The method has the advantage of leading to fragility estimates together with its confidence band (e.g., plus/minus one/two standard deviations from the median). The case-study structure consists of the central frame of an existing moment resisting RC school building (see [14] for more details) constructed in the 1960s, and designed for gravity loads only. A large set of ground-motion containing 160 records [14] has been employed to perform the nonlinear dynamic analysis procedures MCA and IDA, and to estimate the fragility curves considering structural modeling uncertainties. Moreover, MCA and IDA have been carried out also on the two sub-sets (out of the set of 160 records) of 50 and 30 ground motion records, respectively.

2. Methodology

2.1 The Intensity Measure and the Structural Performance Variable

The critical demand to capacity ratio for a prescribed limit state (*LS*, [15]), denoted as DCR_{LS}, has been adopted as the structural performance variable. DCR_{LS} is defined as the demand to capacity ratio for the

component or mechanism that brings the system closer to the onset of the *LS*. DCR_{LS} is always equal to unity at the onset of limit state, and is defined as:

$$DCR_{LS} = \max_j^N \left(\frac{D_j}{C_j(LS)} \right) \quad (1)$$

where N is the number of components; D_j is the demand evaluated for the j^{th} component; $C_j(LS)$ is the capacity for the j^{th} component for the limit state *LS* (weakest link formulation). Three discrete *LS*'s are evaluated according to the Italian Building Code NTC 2018 [18], namely, damage (*SLD*), life safety (*SLV*), and near collapse (*SLC*). The *SLC* regarding ductile failure modes is defined as the point on the lateral force-deformation response in which a 20% drop in resistance has taken place. The onset of the *SLV* is defined on the member force-deformation curve as point with a deformation equal to $3/4^{th}$ of that for the onset of *SLC*. The onset of *SLD* is defined as the point on the force-deformation curve of the component that corresponds to yielding. The onset of *Collapse* limit state for each member is represented by its axial load failure or reaching its ultimate post-capping chord rotation (see [14] for more details).

2.2 The sampling techniques and the "observed data" **D**

Two different sampling techniques have been used to simulate the uncertain modelling parameters from their distributions, namely Monte Carlo simulation (MCS) and Latin Hypercube Sampling (LHS, [19]). LHS is a special type of MCS, which uses the stratification of the theoretical probability distribution functions of input random variables. Herein, we used one of the most efficient strategies to perform sample selection in LHS, which is the sampling of interval mean values (see a comprehensive discussion in [20]). The sampling from each interval is done only once during the simulation. The generation of the LHS is then completed by randomly pairing (without replacement) the resulting values for each of the random variables. In spite of high efficiency of the LHS technique, there are generally two issues concerning statistical correlation [16]: first, diminishing undesired and spurious correlation between random variables generated during sampling procedure (particularly in the case of small number of simulations); second, introducing the prescribed statistical correlations between pairs of random variables. Hence, in order to impose a prescribed correlation matrix into the sampling scheme, an optimization problem for minimizing the difference between the target correlation and actual correlation matrices should be solved. To have opportunity to escape from local minima and finally find the global minimum, a stochastic optimization approach called Simulated Annealing (SA) technique has been recently proposed [16]. Let vector $\boldsymbol{\theta}$ represent all the uncertain modelling parameters including parameters related to component capacity models, construction details and mechanical material (note that we do not consider fragility model parameters and the ground motion representation uncertainties in $\boldsymbol{\theta}$). Each record is applied to a different realization of the vector $\boldsymbol{\theta}$ (i.e., the one-to-one assignment [13, 14, 17]); thus, the number of structural analyses is equal to the number of records in the database, which in turn is equal to the number of structural model realizations. Each realization of the vector $\boldsymbol{\theta}$ (plausible structural model) subjected to a record in the database leads to the corresponding *DCR* value. The set of pairs consisted of *DCR* values for a given limit state and the corresponding ground-motion intensity measure (herein, spectral acceleration at the first-mode period, $S_a(T_1)$), denoted as (DCR_{LS}, S_a) are considered as "observed data **D**" in order to update the probability distribution for the parameters of the prescribed fragility model (e.g., Lognormal).

2.3 Modified Cloud Analysis (MCA)

Let the DCR_{LS} data be partitioned into two parts: (a) *NoC* data which represents the part of the records set for which the structure does not "Collapse", (b) *C* corresponding to the "Collapse"-inducing records (i.e., those records that cause global collapse of the structure; the criteria for selecting these records are comprehensively discussed in [2]). The simple CA is applied to the *NoC* data while the collapse-inducing records are treated separately. This leads to a non-lognormal description of the structural fragility expressed as a weighted average of the (two-parameter) lognormal cumulative distribution describing the non-collapse-inducing records and unity (i.e., the probability of exceeding a *LS* given collapse has taken place). The weights (which sum to unity) are the probability of non-collapse given the intensity level, $P(NoC|S_a)$, and the

probability of collapse given the intensity level (1-$P(NoC|S_a)$), which is defined by a bi-parametric logistic regression model. The structural fragility for a prescribed *LS*, expressed with respect to *NoC* and *C* data, is shown as follows: (see [2] for the derivation):

$$P\left(DCR_{LS}>1\middle|S_a,\boldsymbol{\chi}\right)=\Phi\left(\frac{\ln\eta_{DCR|S_a,NoC}}{\beta_{DCR|S_a,NoC}}\right)\cdot\underbrace{\frac{e^{-(\alpha_0+\alpha_1\ln(S_a))}}{1+e^{-(\alpha_0+\alpha_1\ln(S_a))}}}_{P(NoC|S_a)}+\underbrace{\frac{1}{1+e^{-(\alpha_0+\alpha_1\ln(S_a))}}}_{1-P(NoC|S_a)} \tag{2}$$

where $\eta_{DCR|Sa,NoC}$ and $\beta_{DCR|Sa,NoC}$ are conditional median and logarithmic standard deviation of DCR_{LS} for *NoC* portion of the data; α_0 and α_1 are the parameters of the logistic regression model; Φ is the standardized normal cumulative density function. The median $\eta_{DCR|Sa,NoC}$ for a prescribed *LS* is described as a power-law function of the seismic intensity level *Sa*, i.e., $\eta_{DCR|Sa,NoC}=a\times S_a{}^b$. Eq. (2) illustrates a five-parameter fragility model whose model parameters can be denoted as $\boldsymbol{\chi}=[\ln a,\ b,\ \beta_{DCR|Sa,NoC},\ \alpha_0,\ \alpha_1\ ]$; i.e., given $\boldsymbol{\chi}$, the fragility can be estimated (for simplicity, $\beta_{DCR|NoC,Sa}$ is replaced with $\beta_{DCR|Sa}$ hereafter). Among the five parameters in the MCA-based fragility model, three parameters are from the simple CA and the two other parameters derive from logistic model. The p^{th} percentile of DCR given intensity measure, denoted as DCR^p, can be expressed as (see [2, 21] for the derivation):

$$DCR^p\left(IM\right)=\eta_{DCR|S_a,NoC}\left(IM\right)\cdot\exp\left(\beta_{DCR|S_a}\cdot\Phi^{-1}\left[p/P(NoC\,|\,S_a)\right]\right) \tag{3}$$

where Φ^{-1} is the inverse function of standardized normal distribution. For example, Eq.(3) can estimate the 16^{th}, 50^{th} and 84^{th} percentile curves of *DCR* given S_a.

2.4 IDA Analysis

The structural fragility can also be expressed, in an *IM*-based manner, as the cumulative distribution function for the *IM* values that mark the limit state threshold. Taking advantage of the *IM*-based fragility definition and assuming that the critical S_a values at the onset of the *LS* denoted by $S_a{}^{DCR=1}$ are Lognormally distributed, the structural fragility based on IDA procedure can be calculated as:

$$P\left(DCR_{LS}\geq 1\,|\,S_a=x\right)=P\left(S_a{}^{DCR=1}\leq x\right)=\Phi\left(\frac{\ln x-\ln\eta_{S_a|DCR=1}}{\beta_{S_a|DCR=1}}\right) \tag{4}$$

where $\eta_{Sa|DCR=1}$ and $\beta_{Sa|DCR=1}$ are the median and (logarithmic) standard deviation of the spectral acceleration values $S_a{}^{DCR=1}$ at the onset of *LS*.

2.5 Robust fragility assessment (using simulation)

The Robust Fragility [2, 7, 14] is defined as the expected value for a prescribed fragility model considering the joint probability distribution for the fragility model parameters $\boldsymbol{\chi}$. The Robust Fragility can be expressed as:

$$P\left(DCR_{LS}>1\middle|S_a,\mathbf{D}\right)=\int_{\Omega_\chi}P\left(DCR_{LS}>1\middle|S_a,\boldsymbol{\chi}\right)f(\boldsymbol{\chi}|\mathbf{D})\,\mathrm{d}\boldsymbol{\chi}=\mathrm{E}_{\boldsymbol{\chi}}\left[P\left(DCR_{LS}>1\middle|S_a,\mathbf{D},\boldsymbol{\chi}\right)\right] \tag{5}$$

where $\boldsymbol{\chi}$ is the vector of fragility model parameters (see Section 2.4) and $\Omega_{\boldsymbol{\chi}}$ is its domain; $f(\boldsymbol{\chi}|\mathbf{D})$ is the joint probability distribution for fragility model parameters given the vector of data **D**; $P(DCR_{LS}>1|S_a,\boldsymbol{\chi})$ is the fragility model given the vector $\boldsymbol{\chi}$ (see Eq. 2). $\mathrm{E}_{\boldsymbol{\chi}}(\cdot)$ is the expected value over the vector of fragility parameters $\boldsymbol{\chi}$. Based on the definition represented in Eq. (5), the variance $\sigma^2_{\boldsymbol{\chi}|\mathbf{D}}$ in fragility estimation (to be used to estimate a confidence interval of for the fragility) can be calculated as:

$$\sigma^2_{\boldsymbol{\chi}|\mathbf{D}}\left[P\left(DCR_{LS}>1\middle|S_a,\boldsymbol{\chi}\right)\right]=\mathbb{E}_{\boldsymbol{\chi}|\mathbf{D}}\left[P\left(DCR_{LS}>1\middle|S_a,\boldsymbol{\chi}\right)^2\right]-\left(\mathbb{E}_{\boldsymbol{\chi}|\mathbf{D}}\left[P\left(DCR_{LS}>1\middle|S_a,\boldsymbol{\chi}\right)\right]\right)^2 \tag{6}$$

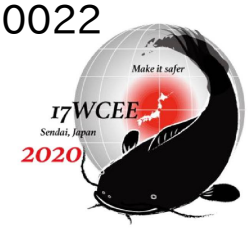

3. Numerical application

3.1 Case study model description

The case-study structure is an existing school building constructed in the 1960s and is designed for gravity loads only. It consists of three stories with a semi-embedded story. The structure lies on soil type B (according to national Italian code NTC 2018 [18] site classification). It is composed of bi-dimensional parallel moment-resisting frames, without transversal beams. The main central frame in the structure is used herein as the structural model. The modelling assumptions and techniques are described in details in [14, 22] (the frame is modelled in OpenSees version 2.5.0, http://opensees.berkeley.edu). To provide a very brief description, the total lateral force-deformation response of the element is derived as follows. First, a detailed moment-curvature analysis is performed and the corresponding response is idealized by a spring. This spring is acting in series with a shear spring and a spring representing the fixed-end rotations due to bar-slip. Second, the total lateral force-deformation response of the element --derived based the interaction between the shear, bar-slip, and the axial-flexural response -- is further modified to account for abrupt degradation due to shear failure. Finally, the post-capping displacement limit is properly estimated based on the type of the member being beam or column; see [14] for more details). The total lateral force-deformation response is used as an input for a distributed plasticity model in OpenSees.

3.2 Ground-motion record selection

A large set of ground-motions including 160 records (for more details, see [14] and its supplemental electronic material) is selected for performing MCA and IDA. These records correspond to soil types B and C (based on NTC 2018 [18] soil classification) having moment magnitude greater than 5 (no limits on the source-to-site distance is considered), and crustal focal mechanisms (reverse, strike-slip and normal faulting styles). Later, two subsets are extracted from the original set of 160 records. A subset of 50 records for MCA were chosen considering the following criteria: (a) the selected records cover a vast range of spectral acceleration values; (b) the records are selected in a way that a significant proportion of records have DCR_{LS} greater than unity; (c) no more than two records from each earthquake of the original set were selected. The subset of 30 records for IDA is established following the *Cloud to IDA* procedure [23], with the objective of limiting excessive scaling of records within the IDA procedure. The procedure is implemented based on the CA results for *SLV* limit state (see [23] for more details). A confidence interval is defined around the intersection of the median of the Cloud data (i.e., the linear regression line in the logarithmic scale) with the line DCR_{SLV}=1 in order to select the records that are going to be subjected to a least amount of scaling.

3.3 The uncertain parameters **θ**

The uncertainty in the modelling parameters are classified as the uncertainties in component capacity models, mechanical material properties, and construction details.

3.3.1 The uncertainty in the component capacity models

Component capacities are modelled as the product of predictive formulas η_C and unit-median lognormal variables ε_C (with logarithmic standard deviation equal to β_C) accounting for the uncertainty in component capacity (as described in [7, 14, 15]). The deviations ε_C from the predictive formulas are fully correlated across the entire frame for each type and independent between different types. Herein, the uncertainties related to the following three capacity predictive models are considered (see [14] for more details): (1) shear resistance V_n according to the model proposed by [24] with β_{C1}=0.19; (2) the displacement δ_{AFL} marking the displacement corresponding to the loss of load bearing capacity proposed by [25] with β_{C2}=0.26; (3) the post-capping rotation θ_{PC} proposed by [26] with β_{C3}=0.72. The median value η_C for each capacity model is equal to its nominal value.

3.3.2 The uncertainty in the mechanical material properties and in the construction details

The uncertain parameters considered for modelling the concrete and steel mechanical properties are illustrated in Table 1. The concrete compressive resistance for the floors (denoted as f'_{c1}, f'_{c2}, f'_{c3}) are

considered jointly lognormally distributed (it has been assumed that the fourth floor has the same material properties as the third floor). The average properties for concrete resistance for each floor are updated using Bayesian updating based on the available destructive and nondestructive in-situ tests for each floor of the case study building (see [27] for more details). The prior distribution for median concrete strength is taken from [28]. In order the estimate the correlation coefficient between the median concrete strength values for each floor, an exponential autoregressive correlation coefficient is used (see [14] for more details). The statistics for the concrete ultimate strain, ε_{cu}, in Table 1 are taken as the model code recommended values (NTC 2018, [18]). There was only one tensile stress test available for steel rebar yielding strength, f_y, and ultimate strength, f_{su}. Nevertheless, this one data point has been used for steel yielding strength as the median, and the COV was chosen from literature results reporting steel property statistics based on the year of construction [29]. The ultimate strength f_{su} is assumed to be fully correlated with f_y. The steel strength has been assumed to be constant throughout the building. The ultimate strain for steel, ε_{su}, has been assigned based on the values recommended in the literature (see [14]).

The uncertainty in the construction details are shown in Table 2. Stirrup spacing in the beams and columns and the concrete cover have assumed to be the most significant sources of uncertainty related to construction details. Having a presumably shear-critical structure, the spacing of the shear rebar is expected to affect significantly the seismic structural behavior. It is assumed that the information about the shear rebar is limited to the knowledge of stirrup diameter (equal to 6 mm), and the intervals in which the stirrup spacing is supposed to vary (the minimum values for stirrup spacing are equal to those specified in the original design documents, and maximum values are loosely based on the maximum admissible stirrup spacing according to the code). Hence, a uniform distribution is assumed. With respect to the uncertainties in concrete cover, it has been assumed to be constant throughout the building. A truncated lognormal distribution is fit to the in situ Geo-Radar test results for the building (see [14]), so that the plausible values for cover thickness are limited to the interval between 25 and 50mm. The nominal values for each parameter are reported in the last column of Table 2.

Table 1: Material Mechanical Properties [14]

Mechanical property		Prior distribution			Posterior distribution			Nominal
		Type	Parameters		Type	Parameters		
Concrete	f'_{c1}	LN (median, COV)	16.5 MPa	0.15	LN (median, COV); systematic over floor; correlated(1) (Figure 3)	20.0 MPa	0.072	20.0 MPa
	f'_{c2}		16.5 MPa	0.15		17.5 MPa	0.068	17.5 MPa
	f'_{c3}		16.5 MPa	0.15		19.2 MPa	0.065	19.2 MPa
	ε_{cu}				LN (median, COV) for all members	0.0035	0.15	0.0035
Steel	f_y	LN	320 MPa	0.08	LN (median, COV); fully correlated for all members	296 MPa	0.08	296 MPa
	f_{su}					435 MPa	0.08	435 MPa
	ε_{su}				Normal (mean, COV); for all members	0.18	0.09	0.18

Table 2: The uncertainty in spacing of shear reinforcement and concrete cover [14]

Defect	Distribution	Value	Nominal
Spacing of shear reinforcement (s)	Uniform	s_c = [200, 400] mm (for all columns) s_{b12} = [150, 350] mm (beams in 1st and 2nd floors) s_{b34} = [200, 400] mm (beams in 3rd and 4th floors)	s_c = 200 mm s_{b12} = 150 mm s_{b34} = 200 mm
Concrete cover	Truncated LN	median = 32.50 mm, COV=0.25, interval = [25, 50] mm systematic for all members	30 mm

3.4 Nonlinear dynamic analyses procedures and fragility estimation

Figs. 1(a,b,c) demonstrate the results of the MCA for the three *LS*'s in the logarithmic scale when the structural modelling uncertainties are not considered. The set of 50 records, described in Section 3.2, is applied to the nominal structural model values and the resulting Cloud data pairs containing DCR_{LS} and the intensity measure $IM=S_a(T_1)$ are estimated for the *SLD, SLV* and *SLC* limit states. The *NoC* data pairs are plotted as blue circles and the *C* data pairs are plotted with red circles. The figures show in dash-dotted light grey line the linear regression fitted in the logarithmic scale to the *NoC* portion of the data (labelled as CA regression). The figures also show the median prediction (DCR^{50th}, plotted as solid grey line) and DCR^{16th} and DCR^{84th} percentiles plotted as grey dashed lines based on both linear and logistic regressions considering the *C* portion of data (see Eq. 3). The MCA-based model parameters χ are shown for each limit state in Figure 1. The median *IM* at the onset of the *LS*, $\eta_{IM|DCR=1}$ (i.e., the median of the fragility) can be obtained by finding the intensity value corresponding to unity from the median performance curve DCR^{50th} (as shown in Figure 1). The logarithmic standard deviation (dispersion) $\beta_{IM|DCR=1}$ can be estimated as half of the logarithmic (vertical) distance between the 16th and the 84th percentile curves (i.e., DCR^{16th} and DCR^{84th}) measured at $DCR_{LS}=1$. As shown in Eq. (2), the MCA-based structural fragility is not a lognormal distribution; it is a 5-parameter distribution. However, the two parameters $\eta_{IM|DCR=1}$ and $\beta_{IM|DCR=1}$ estimated above can be interpreted as the two parameters (median and dispersion, respectively) of an equivalent lognormal distribution. Figs. 2(a,b,c) show the IDA procedure results, performed for the suite of 30 records (described in Section 3.2). The IDA curves are plotted in thin grey lines. Each curve shows the variation in the performance variable DCR_{LS} for a given record as a function of the intensity measure $IM=S_a(T_1)$, while the record's amplitude is linearly scaled-up. The grey dot at the end of each IDA curve denotes the last S_a level before numerical non-convergence or global collapse (i.e., "Collapse" case) associated with the ground motion takes place. The S_a values on the IDA curves corresponding to $DCR_{LS}=1$, denoted as $S_a^{DCR=1}$ (i.e., the intensity levels marking the onset of the limit state, see Eq. 4) are shown as red stars. The histogram of $S_a^{DCR=1}$ data together with the fitted (Lognormal) probability density function (PDF), plotted as a black solid line, are also shown in Fig. 2. The median, $\eta_{IM|DCR=1}$, and (logarithmic) standard deviation, $\beta_{IM|DCR=1}$, of the lognormal PDF is also shown. Figs 3(a,b,c) show the MCA-based Robust Fragility curves (Eq. 5, black solid line) together with plus/minus two standard deviation confidence interval (Eq. 6, grey area) obtained by employing the 50 records for the three *LS*'s. The MCA-based Robust Fragility confidence interval obtained from 50 records for both *SLV* and *SLC* limit states can properly include the MCA-based fragility curves of 160 records (grey dashed line), IDA-based fragility of 160 records (red dashed line), and also IDA-based fragility from 30 records (red solid line). A different discussion is needed for the serviceability limit state *SLD*. In fact, the selection of both the two subsets of 50 and 30 records for MCA and IDA, as well as the initial record selection of 160 records, is based on meeting the recommendations of the record selection for an ultimate limit state. Therefore, these selections work properly for the ultimate limit states (i.e., *SLV* and also *SLC*), since these two ultimate *LS*'s are strictly related. However, fragilities based on these record sets cannot properly take care of the *SLD* which is a service limit state and a kind of "distant" from *SLV*. Figs 4(a,b,c) and Figs 5(a,b,c) show the MCA procedure considering also modelling parameter uncertainties based on both simulation techniques MCS and LHS (with SA) for the 50 records set, and for the three limit states. All the curves are based on the one to one association of records and samples. Figs 6(a,b,c) and 7(a,b,c) show the IDA results, performed for the suite of 30 records. The IDA procedures in these figures consider also modelling parameter uncertainties based on both simulation techniques MCS and LHS (with SA).

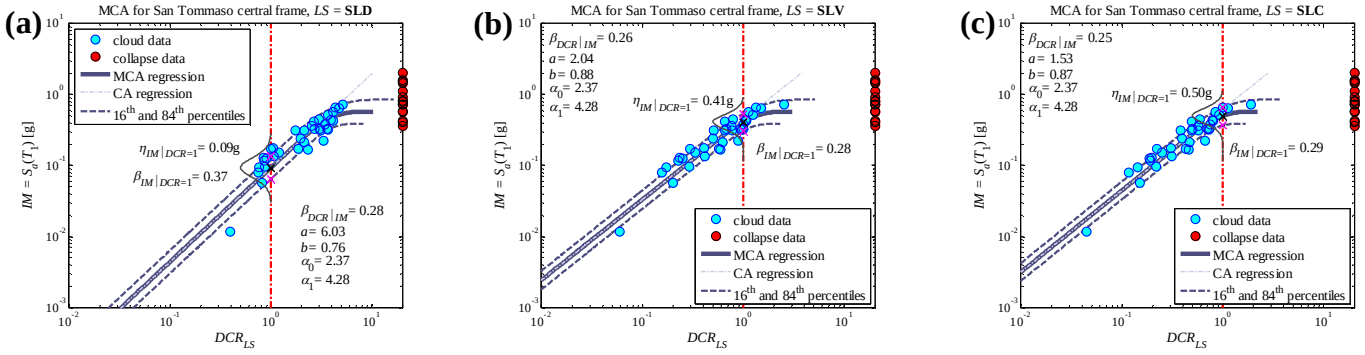

Fig. 1 – Cloud 50 records without uncertainties propagations for the three LSs

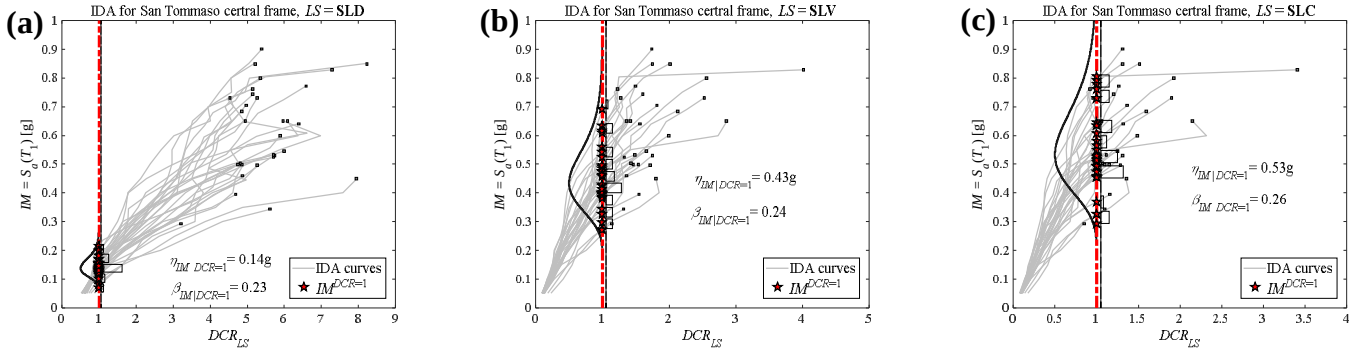

Fig. 2 – IDA 30 records without uncertainties propagations for the three LSs

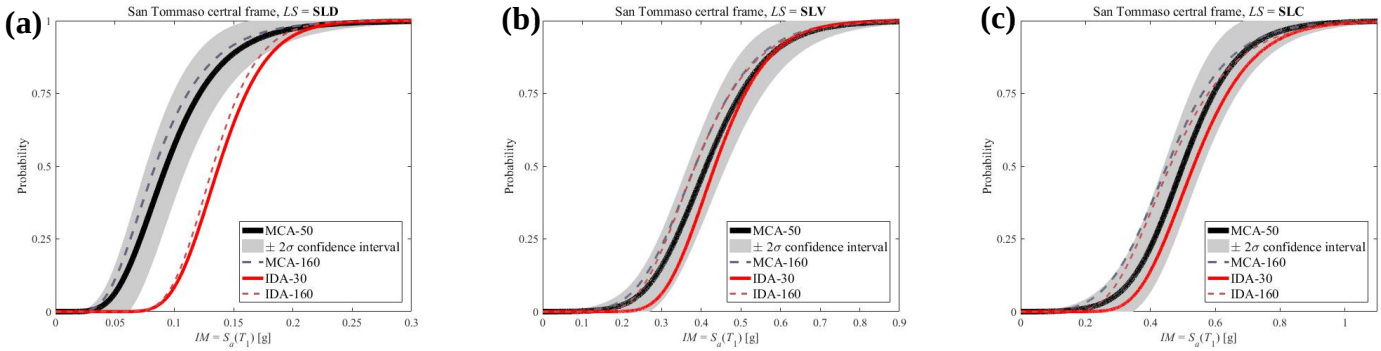

Fig. 3 – Fragility curves comparisons without uncertainties propagations for the three LSs

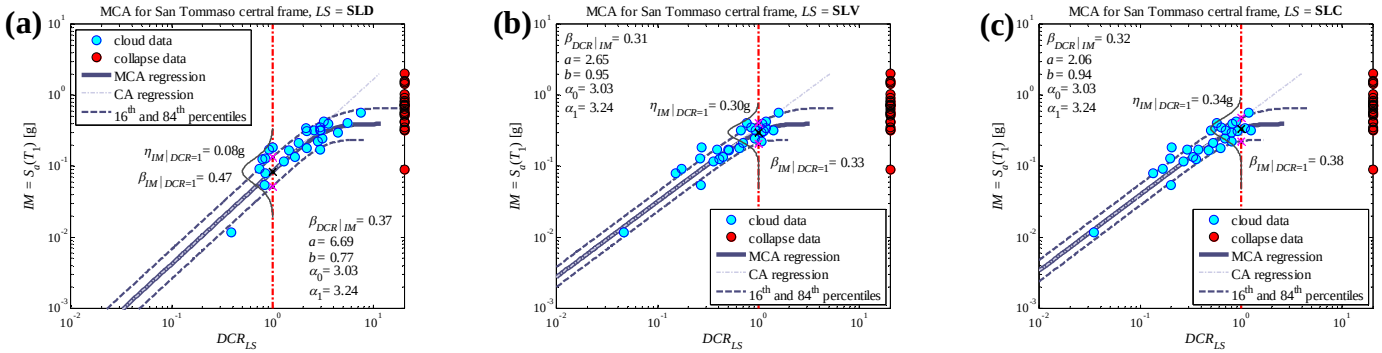

Fig. 4 – Cloud 50 records with uncertainties propagations based on MCS for the three LSs

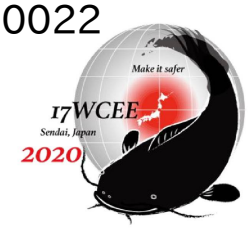

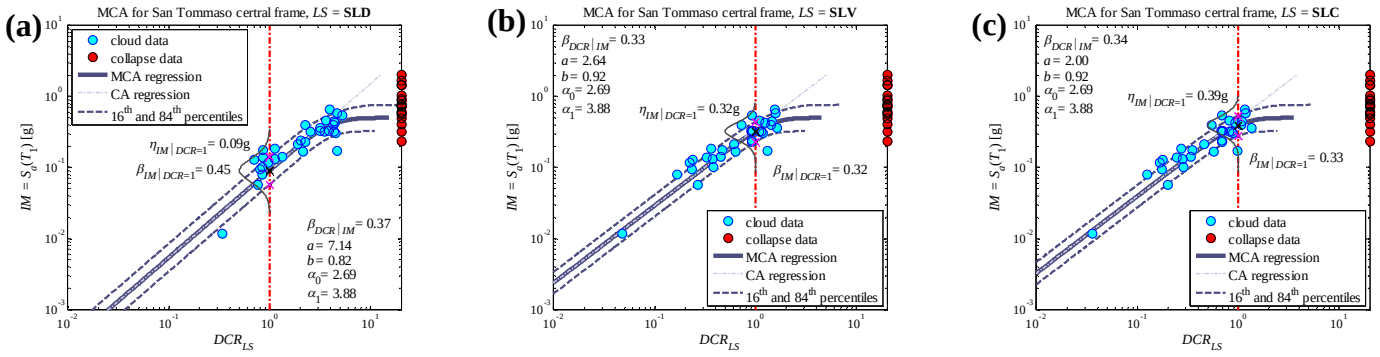

Fig. 5 – Cloud 50 records with uncertainties propagations based on LHS for the three LSs

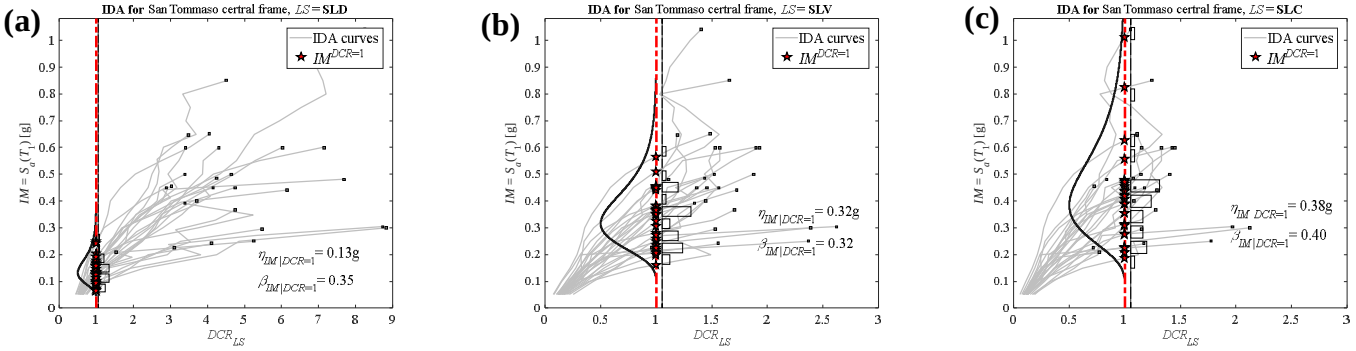

Fig. 6 – IDA 30 records with uncertainties propagations based on MCS for the three LSs

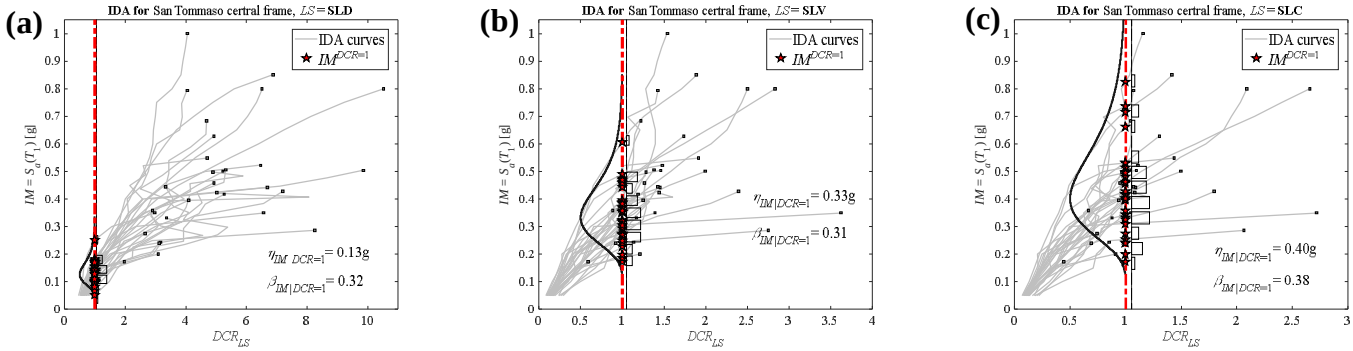

Fig. 7 – IDA 30 records with uncertainties propagations based on LHS for the three LSs

Figs 8(a,b,c) and Figs 9(a,b,c) show the MCA-based Robust Fragility curves and their plus/minus two standard deviation interval obtained by employing the 50 records (considering epistemic uncertainties based on MCS and LHS, as shown in Fig. 4 and Fig. 5) in black solid line and the corresponding confidence intervals marked by grey area. Similar to Fig. 3, the MCA-based Robust Fragility curves (both for MCS and LHS) obtained based on 50 records for both *SLV* and *SLC* limit states include IDA-based fragility of 160 records (red dashed line), and also IDA-based fragility from 30 records (red solid line). The MCA-based fragility of 160 records (black dashed line) presents a certain shift in terms of median and dispersion with respect to the other curves. It reveals that the response for MCA is different when the number of samples is respectively 50 and 160. This is because the cases with 160 records/simulations show a large number of "collapse" cases taking place for rather weak records (i.e., very weak structural models collapsed for very low levels of S_a) and there is also larger dispersion in the regression residuals for the *NoC* records. These cases are relative to very weak structural models (e.g., very large stirrups spaces with low values of concrete and shear resistance). The probability of having these cases with 50 records/simulations is lower. The MCA-based fragility for the set of 50 records (dotted-black line) and IDA-based fragility for the set of 30 records (dotted-red line), considering no epistemic uncertainties, are also shown in Fig. 8 and Fig. 9. As confirmed in

the previous research ([9, 14]), consideration of both R2R variability and structural modelling uncertainties leads to a reduction in the median of the fragility curves with respect to the fragilities considering only the R2R variability.

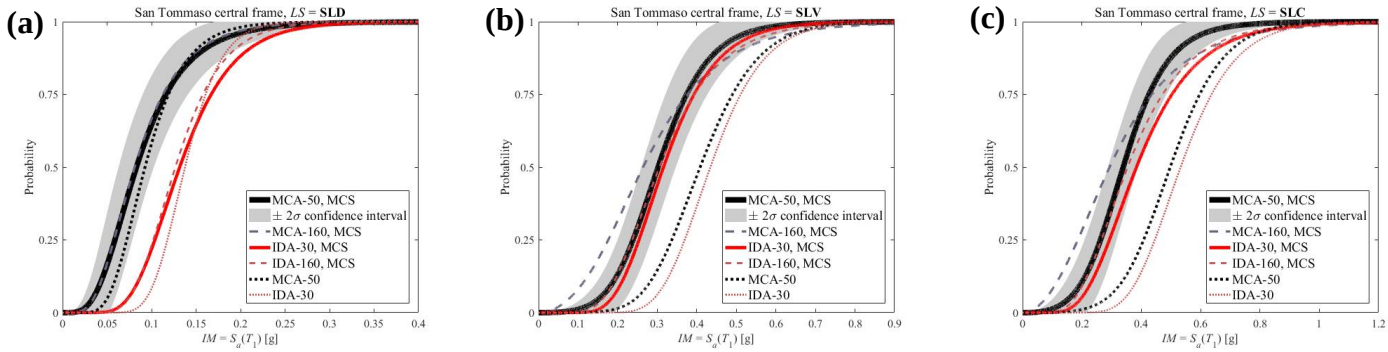

Fig. 8 – Fragility curves comparisons with uncertainties propagations based on MCS for the three LSs

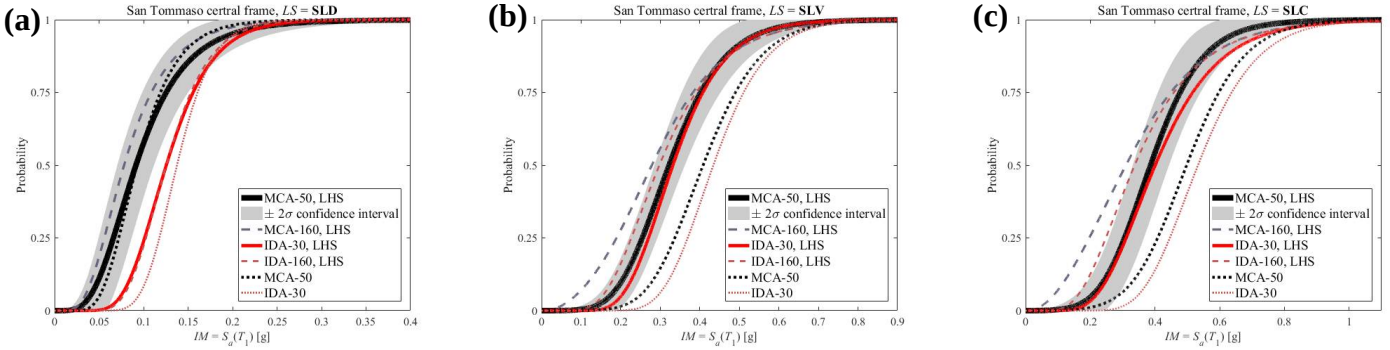

Fig. 9 – Fragility curves comparisons with uncertainties propagations based on LHS for the three LSs

4. Conclusions

It is observed that MCA and IDA-based fragility curves with the consideration of both R2R variability and structural modelling uncertainties manifest a reduction in the median with respect to the cases where only the R2R variability is considered. Moreover, it can be noted that the MCA and IDA lead to reasonably close agreement in terms of fragility for the ultimate limit states. However, a net shift between the two methods is observed for the service limit state. This can be partially attributed to the fact that the record selection for MCA is done for the ultimate states and the suite of records does not include a very large number of low-intensity records. It is also seen that the two sets of fragility curves with modelling uncertainties obtained using the LHS and MCS techniques are reasonably close. The fragility curve considering modelling uncertainties based on 160 records seems to be to the left-hand side with respect to those obtained based on 30 and 50 records for the near collapse limit state. This can be both attributed to the large scatter Cloud data around the regression prediction and a large number of very weak buildings experiencing collapse.

5. Acknowledgments

This work has benefitted from the first author's visit period at the National Technical University of Athens (NTUA), which was funded from the Universities for EU Projects contest from SEND consortium. This support is gratefully acknowledged.

6. References

[1] Cornell CA, Krawinkler H (2000): Progress and challenges in seismic performance assessment. PEER Center News, **3** (2): 1-2.

[2] Jalayer F, Ebrahimian H, Miano A, Manfredi G, Sezen H (2017): Analytical fragility assessment using un-scaled ground motion records. *Earthquake Engineering and Structural Dynamics*, **46** (15): 2639-2663.

[3] Vamvatsikos D, Cornell C.A (2002): Incremental dynamic analysis. *Earthquake Engineering and Structural Dynamics*, **31** (3): 491-514.

[4] Vamvatsikos D, Cornell C.A (2004): Applied Incremental Dynamic Analysis. *Earthquake Spectra*, **20**(2): 523-553.

[5] Bazzurro P, Cornell CA, Shome N, Carballo JE (1998): Three proposals for characterizing MDOF nonlinear seismic response. *Journal of Structural Engineering* (ASCE); **124** (11): 1281-1289.

[6] Cornell CA, Jalayer F, Hamburger RO, Foutch DA (2002): Probabilistic basis for 2000 SAC federal emergency management agency steel moment frame guidelines. *Journal of Structural Engineering*, **128**(4), 526-533.

[7] Jalayer F, De Risi R, Manfredi G (2015): Bayesian Cloud Analysis: efficient structural fragility assessment using linear regression. *Bulletin of Earthquake Engineering*, **13**(4): 1183-1203.

[8] Jalayer F, Elefante L, Iervolino I, Manfredi G. (2011): Knowledge-based performance assessment of existing RC buildings. *Journal of Earthquake Engineering*; **15** (3): 362-389.

[9] Miano A, Jalayer F, Prota A. (2017): Considering structural modeling uncertainties using Bayesian cloud analysis. In Proceedings of the 6th ECCOMAS Thematic Conference on Computational Methods in Structural Dynamics and Earthquake Engineering (COMPDYN 2017), 15-17 June 2017, Rhodes Island, Greece.

[10] Vamvatsikos D, Fragiadakis M (2010): Incremental dynamic analysis for estimating seismic performance sensitivity and uncertainty. *Earthquake Engineering and Structural Dynamics*, **39**(2), 141-163.

[11] Celarec D, Dolšek M (2013): The impact of modelling uncertainties on the seismic performance assessment of reinforced concrete frame buildings. *Engineering Structures*, **52**, 340-354.

[12] Jalayer F, Iervolino I, Manfredi G (2010): Structural modeling uncertainties and their influence on seismic assessment of existing RC structures. *Structural Safety*, **32** (3): 220-228.

[13] Franchin P, Ragni L, Rota M, Zona A (2018): Modelling uncertainties of Italian code-conforming structures for the purpose of seismic response analysis. *Journal of Earthquake Engineering*, **22**(sup2):1964-1989.

[14] Jalayer F, Ebrahimian H (2019): Seismic reliability assessment and the nonergodicity in the modelling parameter uncertainties. *Earthquake Engineering and Structural Dynamics.*

[15] Jalayer F, Franchin P, Pinto PE (2007). A scalar damage measure for seismic reliability analysis of RC frames. *Earthquake Engineering and Structural Dynamics*; **36** (13): 2059–2079.

[16] Vorechovsky M, Novak D (2009): Correlation control in small-sample Monte Carlo type simulations. I. A simulated annealing approach. *Probabilistic Engineering Mechanics*, **24**(3), 452–462.

[17] Vamvatsikos D (2014): Seismic performance uncertainty estimation via IDA with progressive accelerogram-wise latin hypercube sampling. Journal of Structural Engineering, **140**(8):A4014015-1-10.

[18] NTC 2018 Commentary (2019): Supplemento ordinario alla Gazzetta Ufficiale, n. 35 del 11 Febbraio 2019. Ministero delle Infrastrutture e dei Trasporti, Circolare 21 Gennaio 2019 “Istruzioni per applicare dell'Aggiornamento delle Norme tecniche per le costruzioni» di cui al decreto ministeriale 17 Gennaio 2018” (in Italian).

[19] Helton JC, Davis FJ (2002): Latin Hypercube Sampling and the propagation of uncertainty in analyses of complex systems. Tech. Rep. SAND2001-0417, Sandia National Laboratories Albuquerque, New Mexico (Livermore, CA).

[20] Ebrahimian H, De Risi R (2014): Seismic reliability assessment, alternative methods for. Encyclopedia of Earthquake Engineering (book chapter). Editors: Michael Beer, Ioannis A. Kougioumtzoglou, Edoardo Patelli, Ivan Siu-Kui Au, Springer-Verlag Berlin Heidelberg 2014, pp 2957-2981. DOI: 10.1007/978-3-642-36197-5_245-1. ISBN: 978-3-642-36197-5.

[21] Jalayer, F (2003): Direct probabilistic seismic analysis: implementing non-linear dynamic assessments, Ph.D. Thesis, Stanford University, CA.

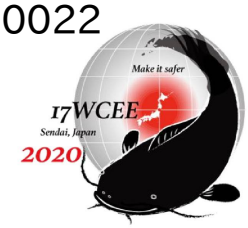

[22] Jalayer F, Ebrahimian H, Miano A (2019): N2 with Cloud: A non-linear dynamic analysis procedure for the equivalent SDOF system. In *Proceedings of XVIII Conference ANIDIS of seismic engineering in Italy (ANIDIS 2019)*. Ascoli Piceno, Italy, 15-19 September 2019.

[23] Miano A, Jalayer F, Ebrahimian H, Prota A (2018): Cloud to IDA: efficient fragility assessment with limited scaling. *Earthquake Engineering and Structural Dynamics*, **47**(5):1124-1147.

[24] Biskinis DE, Roupakias GK, Fardis MN (2004): Degradation of shear strength of reinforced concrete members with inelastic cyclic displacements. *ACI Structural Journal*, **101**(6):773-783.

[25] Elwood KJ, Moehle JP (2005): Axial capacity model for shear-damaged columns. *ACI Structural Journal*, *102*(4):578-587.

[26] Haselton CB, Liel AB, Lamge ST, Deierlein GG (2008): Beam-column element model calibrated for predicting flexural response leading to global collapse of RC frame buildings. PEER Report 2007/03, Pacific Earthquake Engineering Research Center, University of California, Berkeley.

[27] Ebrahimian H, Jalayer F (2019): In-situ tests and inspections for reliability assessment of RC buildings: how accurate? In Proceedings of XVIII Conference ANIDIS of seismic engineering in Italy (ANIDIS 2019). Ascoli Piceno, Italy, 15-19 September 2019.

[28] Verderame GM, Manfredi G, Frunzio G. (2001): Le proprietà meccaniche dei calcestruzzi impiegati nelle strutture in cemento armato realizzate negli anni'60. *X Congresso Nazionale "L'ingegneria Sismica in Italia"*, Potenza – Matera 9-13 settembre 2001 (in Italian).

[29] Verderame GM, Stella A, Cosenza E. (2001): Le proprietà meccaniche degli acciai impiegati nelle strutture in cemento armato realizzate negli anni'60. X Convegno Nazionale "L'Ingegneria Sismica in Italia", Potenza e Matera 9-13 Settembre 2001 (in Italian).

